

Mitigating self-action processes with chirp or binary phase shaping

GENNADY RASSKAZOV,¹ ANTON RYABTSEV,¹ VADIM V. LOZOVY,¹ AND MARCOS DANTUS^{1,2,*}

¹Department of Chemistry, Michigan State University, East Lansing, Michigan 48824, USA

²Department of Physics and Astronomy, Michigan State University, East Lansing, Michigan 48824, USA

*Corresponding author: dantus@msu.edu

Received 20 October 2015; revised 19 November 2015; accepted 23 November 2015; posted 1 December 2015 (Doc. ID 252315); published 22 December 2015

We report the use of binary phase shaping to mitigate pulse degradation and self-focusing in fused silica. The results of simulation and estimated mitigation efficiency are supported by experimental results using both chirped and binary phase-shaped pulses. Possible applications are considered. © 2015 Optical Society of America

OCIS codes: (320.5540) Pulse shaping; (320.7090) Ultrafast lasers; (320.7110) Ultrafast nonlinear optics; (320.7140) Ultrafast processes in fibers; (190.5940) Self-action effects.

<http://dx.doi.org/10.1364/OL.41.000131>

Self-action effects in optical beam propagation occur when an electromagnetic field is sufficiently high to induce index of refraction changes in the medium. An intensity-dependent refractive index causes self-focusing and self-phase modulation (SPM) where the one relates to the spatial and the other to the temporal domain. SPM leads to spectral changes [1], and it is found to be useful in such applications as soliton mode-locked laser [2], semiconductor optical amplifiers [3], additive pulse mode-locking systems [4], generation of broadband laser pulses [5,6], and femtosecond fiber oscillators [7]. Self-focusing is found to be useful in Kerr-lens mode-locked lasers [8]. For many other applications, SPM, combined with chromatic dispersion of material and often aggravated by self-focusing, deteriorates pulse quality, causing unwanted spectral and temporal changes and even damage of the medium where the pulse propagates [9,10].

We use a binary phase mask composed of either zeros or π at the Fourier plane of a 4- f shaper [11–13]. The idea of using binary phase shaping (BPS) comes from experiments where it was shown that BPS provides a robust mitigation of nonlinear optical processes [14], and the symmetry of the phase can be used to cause selective nonlinear excitation [15,16]. BPS has been used to control multiphoton excitation-induced chemical reactions [17] and for achieving vibrational mode selectivity in coherent anti-Stokes Raman scattering (CARS) spectroscopy [18]. BPS causes a femtosecond pulse to break into a train of pulses with overall longer duration and lower peak power. It has been shown to increase the transmission distance of laser pulses in an optical fiber [19].

Pastirk *et al.* showed that a binary phase introduced prior to amplification can be compensated for afterward [20]. This concept and its possible applications are illustrated in Fig. 1. We show (a) that a pulse can be stretched in the time domain by a binary phase, then amplified and recompressed by addition of the same binary phase [20]. This fact makes BPS attractive for (b) optical amplification and (c) laser endoscopy.

Self-action mitigation requires a decrease in the laser peak power to a level where induced nonlinearities have no “visible” effect. Such methods include temporal stretching of pulses as in chirp pulse amplification (CPA) systems [21], splitting the pulse into a train of pulses as in divided-pulse amplification [22], and increasing mode area [23]. In general, Ti:Sapphire pulsed laser systems, such as CPA-based systems, stretch the pulses up to 4 orders of magnitude by introducing chirp. An alternative method is to introduce cascaded nonlinearities in a cavity for the compensation of laser-induced phase shift in a medium [24,25]. The difficulty of this method is that it depends on the nonlinearity of the nonlinear crystal, and the amplification gain is orders of magnitude less than in CPA systems [25]. Divided pulse amplification and mode area increases can reduce peak intensity by at most 2 orders of magnitude.

We conducted experiments and numerical simulations on how BPS affects temporal pulse shape. For both experiments and simulations we used the fundamental laser spectrum of

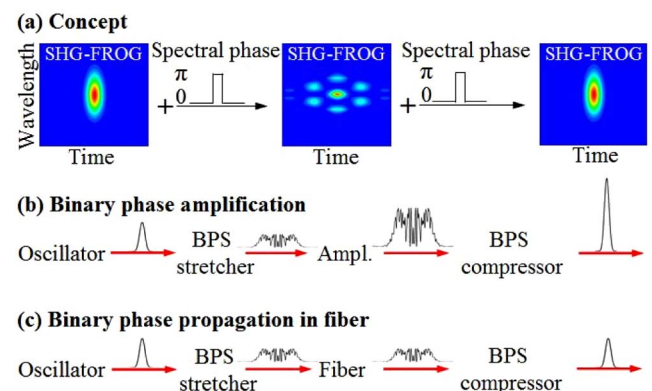


Fig. 1. (a) The concept of using BPS in (b) application to optical amplification systems, and (c) application to fiber lasers.

a Ti:Sapphire amplifier with 40 fs pulse duration FWHM (τ_0) [see Fig. 2(a)]. The spectrum is spread over 600 pixels of spatial light modulator (SLM), as it is in our experiment (explained further). We introduce the term “bit,” which stands for the partition number. Since the spectrum covers 600 pixels, it corresponds to the maximum number of 1-pixel bits. In Fig. 2(a) we show the fundamental spectrum and the optimum 14-bit (600/14 \approx 42 pixels per bit) binary phase out of 16,384 phases to achieve more than an order of magnitude peak intensity reduction in the time domain. To calculate the pulse shape in the time domain we used the Fourier transform:

$$I(t) = \left| \int \sqrt{I(\omega)} e^{i\varphi(\omega)} e^{-i\omega t} d\omega \right|^2, \quad (1)$$

where $I(\omega)$ is the pulse spectrum [red curve in Fig. 2(a)], and $\varphi(\omega)$ is the binary spectral phase [black curve in Fig. 2(a)]. Figure 2(b) compares the time profiles of a transform-limited (TL) pulse, periodic zero/ π and the optimal phase [shown in Fig. 2(a)].

In Fig. 2(c) we show the 128×128 matrix of inversed peak-power ratio values corresponding to all possible 14-bit binary phases. The search space corresponds to the peak-power reduction for each of the different BPS possible. The row and column index of each element is defined by the first and second half of its binary number representation, respectively. In this representation coordinates (0,0) and (128,128) correspond to TL pulses. The global optimum phase with coordinates (65,86) creates 12 times peak power reduction in this case. We find a pattern for the location of the best phases. The pattern is conserved when increasing the number of bits and becomes more

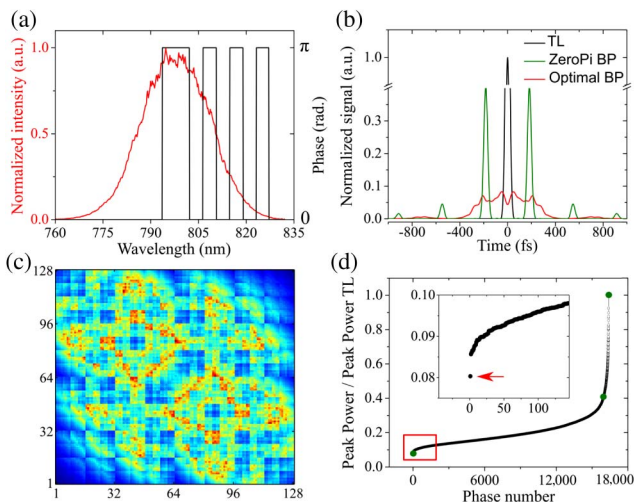


Fig. 2. Effect of BPS for 14-bit binary phases. (a) The red curve corresponds to the laser spectrum; the black line corresponds to the optimum 14-bit phase mask. (b) Comparison between simulated pulse profiles in time domain for TL (black), $0/\pi$ sequence (green), and optimal (red) 14-bit binary phases. Note the break in the vertical axis. (c) Binary phase matrix 128×128 showing inverse peak-power ratio for 14-bit phases. The row and column index of each element is defined by the first and second half of its binary number representation, respectively. Red is best; black is no peak-power reduction. (d) Peak-power ratio values from (c) sorted in ascending order. The green dots correspond to the pulses shown in (b). The red arrow points to the optimal phase.

detailed. Figure 2(d) shows the peak-power ratio values for the 14-bit binary phases sorted in ascending order.

The number of bits needed to decrease the peak power of an ultrafast laser was first explored through numerical simulation. The plot is presented in double logarithmic scale (Fig. 3). All the possible phase combinations were evaluated up to 25 bits; see the region between arrows, fitted with a red dashed line, and smallest peak power normalized on TL peak power is plotted against the corresponding bit number. The smallest peak power was the condition in our algorithm to choose the optimal phase. The slope of the linear fit is -0.95 . The deviation from the linear behavior for the bit number >25 arises from the fact that we did not use the optimal binary phase due to computational resources limit; instead of analyzing all possible phase combinations, only 10^6 of them were analyzed. From the prediction line (red dashed line), it follows that with 1400 bits, one can achieve 1000 times peak-power reduction, which is comparable with stretching applied in CPA systems [26].

For experimental measurements we used a laser system comprising of a Ti:Sapphire oscillator (KM labs), regenerative amplifier (Spitfire, Spectra-Physics, USA) and a pulse shaper (MIIPS HD, BioPhotonic solutions, Inc., USA) with a 2D SLM (792×600 pixels, LCOS-SLM, Hamamatsu, Japan). The laser produces pulses with 40 fs duration with the spectrum shown in Fig. 2(a) centered at 800 nm. After the shaper, the laser beam was focused on a 1 mm fused silica slab placed on a controllable stage, see Fig. 4(a). The laser light was collected by spectrometer (USB 4000, Ocean Optics, USA) through a diffusive surface. We measured self-focusing as a function of chirp (quadratic phase) and for selected binary phases.

Before the measurements, the laser pulses were compressed to TL duration using multiphoton intrapulse interference phase-scan (MIIPS) [27]. The best binary phase for a particular bit number was found out of 10^6 random phase combinations and applied by SLM on top of the compression mask. The fused silica plate was placed on the stage, and a z-scan [28] measurement was performed in order to detect self-focusing. In order to find the chirp-to-bit correspondence, the BPS mask was switched off and the same scan was run at the same average power with different chirp phases to find the chirp value that

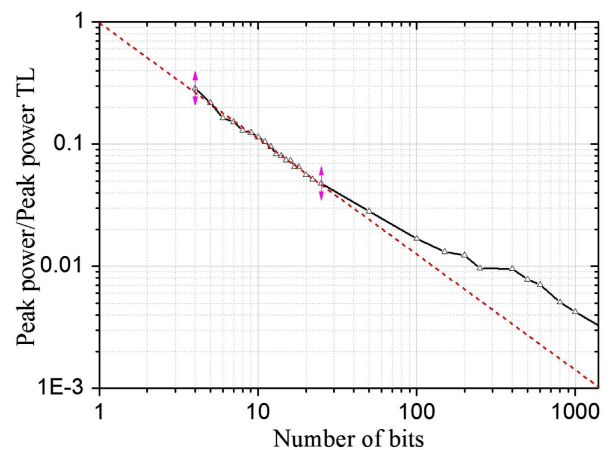


Fig. 3. Simulation of binary phase peak-power reduction for 40 fs pulses. The dependence of normalized peak power versus binary phase in double logarithmic scale. Triangles connected with black line correspond to calculated values. Red line is a fit based on the linear region.

matched the amount of self-focusing for the binary phase. Two such scans are illustrated for chirp ($29.3 \times \tau_0^2 \approx 47,000 \text{ fs}^2$) and binary phase (150-bit phase); see Fig. 4(b) red and black points, respectively. During the experiment we ensured there was no change in the laser spectrum caused by the shaper. The dispersion length of the sample is much greater than the thickness of the slab used; therefore, all the effects relate to nonlinearities.

The same measurements were performed for 25, 50, 100, and 200-bit phases. Figure 4(c), black squares, illustrates the experimental binary phase to chirp correspondence. The red dashed line is the theoretical prediction of binary phase and its chirp equivalent for 40 fs duration pulse. Figure 4(c) shows that the experimental curve follows the behavior of the theoretical curve with deviation as expected, due to the limited number of phases being evaluated.

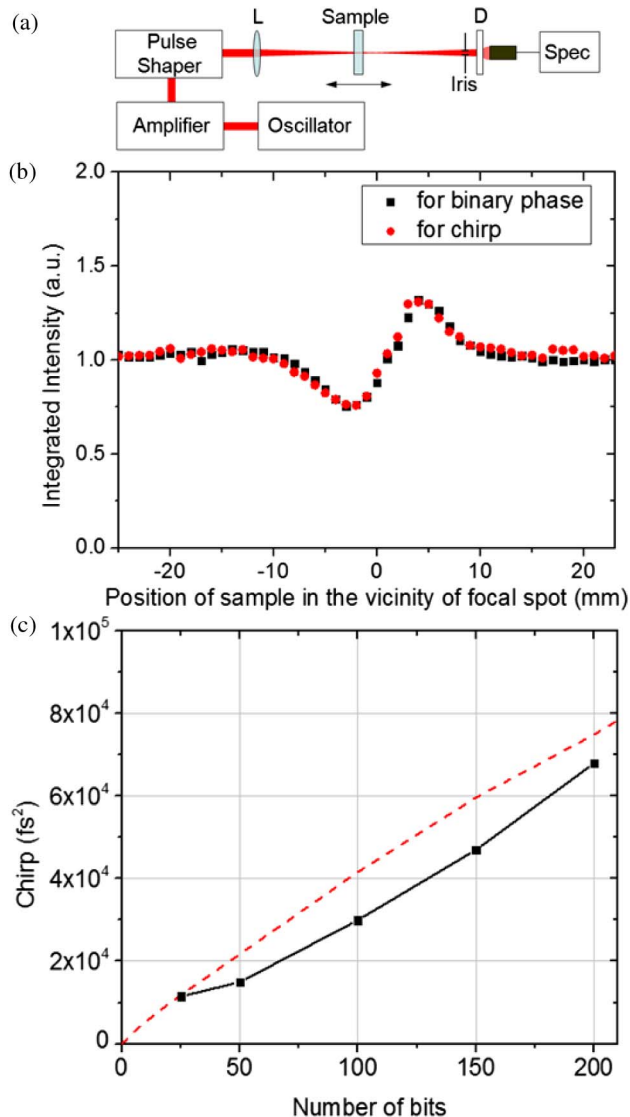


Fig. 4. Experimental results. (a) Experimental setup. L, lens; D, diffruser; (b) integrated signal at different positions of the fused silica window from the focal spot for 150-bit phase, black squares, and chirp value of $\sim 29.3 \times \tau_0^2 \text{ fs}^2$, red circles; (c) experimental bit-to-chirp correspondence (black squares). Red dashed line is a theoretical prediction assuming optimum binary phases.

A significant difficulty involved finding optimum BPS for large number of bits. Optimization algorithms depend on the search space and on knowledge about the optimum solution. Problems such as optimization of the second harmonic signal can be solved quickly because the global optimum is surrounded by promising nearby solutions, i.e., the search space is convex. The other extreme is known as a “needle-in-a-haystack,” for which no method is superior to random search [29,30]. The synthesis of *a priori*-defined temporal pulses has been solved through the combination of genetic algorithms and Fourier-based algorithms [31,32]. However, these approaches require knowledge of the optimum solution. For example, if the optimum pulse should have a flat top temporal profile, the spectral phase required can be directly written without the need for optimization algorithms [33].

In conclusion, we have demonstrated that BPS can be used for self-action processes mitigation. For CPA systems, a large number of bits would be needed; however, SLMs with 12,288 pixels exist (Meadowlark Optics, Colorado). Binary phase modulation could be suitable for laser endoscopy applications, where a fiber-Bragg grating or special multilayer dielectric mirror would accomplish the final compression, for example. We provide the means to estimate how many bits are needed to reduce the peak power for a particular application.

Funding. NSWCRANE (N00164-14-1-1008).

Acknowledgment. The information in this Letter does not necessarily reflect the position or the policy of the government, and no official endorsement should be inferred.

REFERENCES

1. F. Shimizu, Phys. Rev. Lett. **19**, 1097 (1967).
2. L. F. Mollenauer and R. H. Stolen, Opt. Lett. **9**, 13 (1984).
3. G. P. Agrawal and N. A. Olsson, IEEE J. Quantum Electron. **25**, 2297 (1989).
4. E. P. Ippen, H. A. Haus, and L. Y. Liu, J. Opt. Soc. Am. B **6**, 1736 (1989).
5. M. Nisoli, S. De Silvestri, and O. Svelto, Appl. Phys. Lett. **68**, 2793 (1996).
6. C.-H. Lu, Y.-J. Tsou, H.-Y. Chen, B.-H. Chen, Y.-C. Cheng, S.-D. Yang, M.-C. Chen, C.-C. Hsu, and A. H. Kung, Optica **1**, 400 (2014).
7. A. Chong, J. Buckley, W. H. Renninger, and F. W. Wise, Opt. Express **14**, 10095 (2006).
8. D. E. Spence, P. N. Kean, and W. Sibbett, Opt. Lett. **16**, 42 (1991).
9. G. A. Askaryan, Sov. Phys. JETP **15**, 1088 (1962).
10. N. Bloembergen, IEEE J. Quantum Electron. **10**, 375 (1974).
11. C. Froehly, B. Colombeau, and M. Vampouille, in *Progress in Optics*, E. Wolf, ed. (North-Holland, 1983), Vol. **20**, pp. 65–153.
12. A. M. Weiner, J. P. Heritage, and E. M. Kirschner, J. Opt. Soc. Am. B **5**, 1563 (1988).
13. A. M. Weiner, D. E. Leaird, J. S. Patel, and J. R. Wullert, IEEE J. Quantum Electron. **28**, 908 (1992).
14. D. Elyahu, R. A. Salvatore, J. Rosen, A. Yariv, and J. Drolet, Opt. Lett. **20**, 1412 (1995).
15. V. V. Lozovoy, B. Xu, J. C. Shane, and M. Dantus, Phys. Rev. A **74**, 041805(R) (2006).
16. M. Comstock, V. V. Lozovoy, I. Pastirk, and M. Dantus, Opt. Express **12**, 1061 (2004).
17. V. V. Lozovoy, T. C. Gunaratne, J. C. Shane, and M. Dantus, ChemPhysChem. **7**, 2471 (2006).
18. P. Wrzesinski, D. Pestov, V. V. Lozovoy, B. Xu, S. Roy, J. R. Gord, and M. Dantus, J. Raman Spectrosc. **42**, 393 (2011).

19. M. Wichers and W. Rosenkranz, *Optical Fiber Communication Conference*, OSA Technical Digest (Optical Society of America, 2001), paper WDD43.
20. I. Pastirk, B. Resan, J. MacKay, and M. Dantus, *Opt. Express* **14**, 9537 (2006).
21. D. Strickland and G. Mourou, *Opt. Commun.* **56**, 219 (1985).
22. S. Zhou, F. W. Wise, and D. G. Ouzounov, *Opt. Lett.* **32**, 871 (2007).
23. K. Wang and C. Xu, *Opt. Lett.* **36**, 942 (2011).
24. K. Beckwitt, F. W. Wise, L. Qian, L. A. Walker, and E. Canto-Said, *Opt. Lett.* **26**, 1696 (2001).
25. C. Dorrer, R. G. Roides, J. Bromage, and J. D. Zuegel, *Opt. Lett.* **39**, 4466 (2014).
26. M. Pessot, P. Maine, and G. Mourou, *Opt. Commun.* **62**, 419 (1987).
27. Y. Coello, V. V. Lozovoy, T. C. Gunaratne, B. Xu, I. Borukhovich, C.-H. Tseng, T. Weinacht, and M. Dantus, *J. Opt. Soc. Am. B* **25**, A140 (2008).
28. M. Sheik-Bahae, A. A. Said, and E. W. Van Stryland, *Opt. Lett.* **14**, 955 (1989).
29. L. Kallel, B. Naudts, and C. R. Reeves, *Theoretical Aspects of Evolutionary Computing*, L. Kallel, B. Naudts, and A. Rogers, eds. (Springer-Verlag, 2001), pp. 175–206.
30. M. Dantus and V. V. Lozovoy, *Chem. Rev.* **104**, 1813 (2004).
31. M. Hacker, G. Stobrawa, and T. Feurer, *Opt. Express* **9**, 191 (2001).
32. S. Thomas, A. Malacarne, F. Fresi, L. Poti, and J. Azana, *J. Lightwave Technol.* **28**, 1832 (2010).
33. V. V. Lozovoy, G. Rasskazov, A. Ryabtsev, and M. Dantus, *Opt. Express* **23**, 27105 (2015).